Journal of Neural Engineering

PURPOSE-LED PUBLISHING™

PAPER

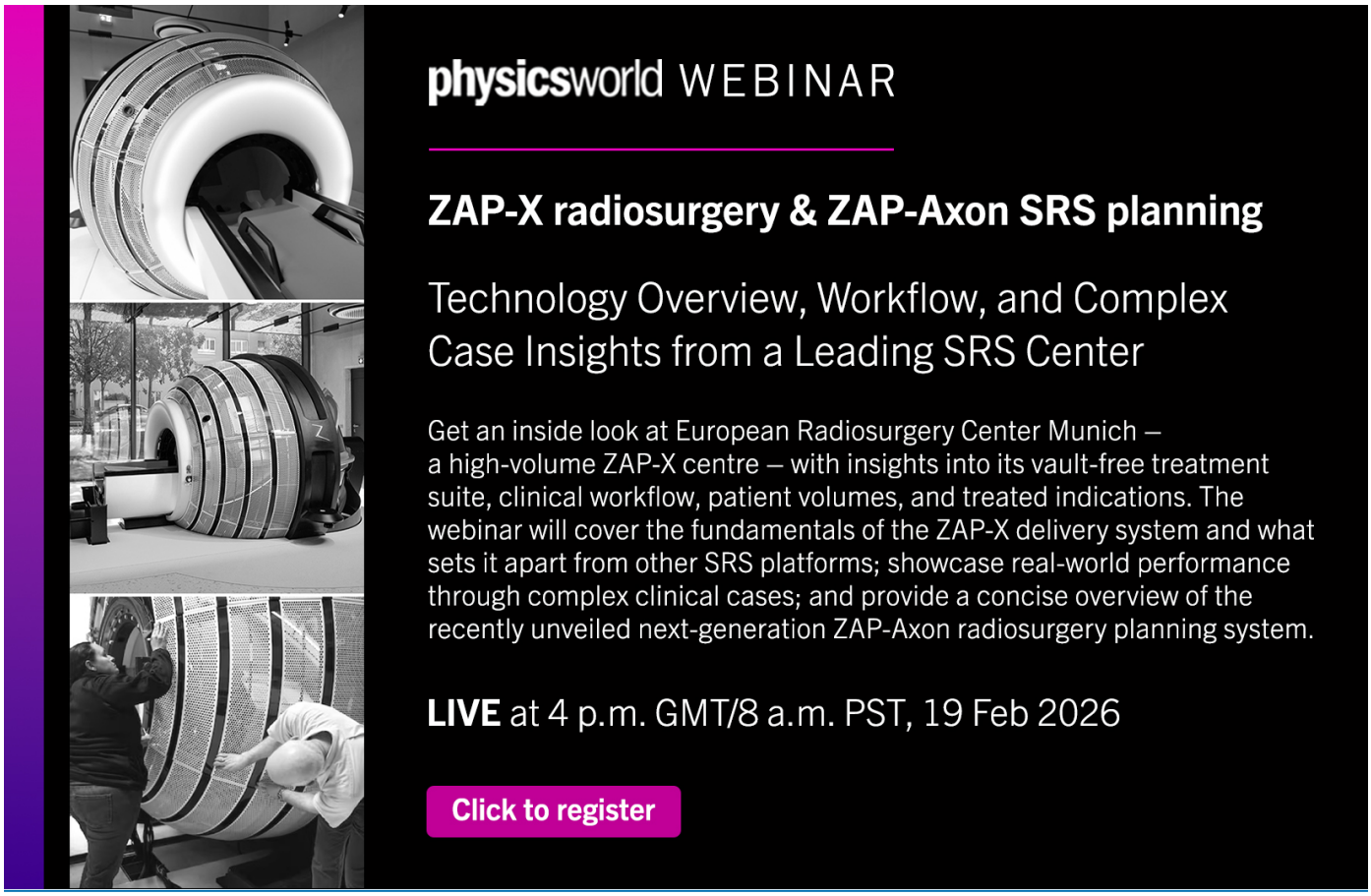
EEG-based meditation decoding: tackling subject variability with spatial and temporal alignment

To cite this article: Angeliki-Ilektra Karaiskou *et al* 2025 *J. Neural Eng.* **22** 066032

View the article online for updates and enhancements.

You may also like

- Lightweight deep learning models for EEG decoding: a review
Yizhen Li, Enze Chen, Xiaolin Xiao et al.
- Determining the relationship of heart rate and blood pressure using voluntary cardio-respiratory synchronization (VCRS)
Lynne I Mason and Robert P Patterson
- Neural correlation between swallowing motor imagery and execution: an EEG analysis
Xiang Qiu, Zhi-Yong Wang, Xiao-Hong Jiang et al.



This content was downloaded from IP address 134.58.253.56 on 27/01/2026 at 10:56

Journal of Neural Engineering

Check for updates

PAPER

RECEIVED
18 April 2025

REVISED
12 November 2025

ACCEPTED FOR PUBLICATION
9 December 2025

PUBLISHED
22 December 2025

EEG-based meditation decoding: tackling subject variability with spatial and temporal alignment

Angeliki-Ilektra Karaiskou[1,2,*], **Carolina Varon**[1], **Cem Ates Musluoglu**[1], **Kaat Alaerts**[2,4] and **Maarten De Vos**[1,3,4]

[1] STADIUS Center for Dynamical Systems Signal Processing and Data Analytics, Department of Electrical Engineering (ESAT), KU Leuven, 3001 Leuven, Belgium
[2] Research Group for Neurorehabilitation, Department of Rehabilitation Sciences, KU Leuven, 3001 Leuven, Belgium
[3] Department of Development and Regeneration, KU Leuven, 3001 Leuven, Belgium
[4] Joint senior authors.
[*] Author to whom any correspondence should be addressed.

E-mail: angeliki.karaiskou@kuleuven.be

Keywords: electroencephalography, domain adaptation, deep learning, Riemannian geometry, Monge map, meditation, brain–computer interface

Abstract

Objective. Meditation and mindfulness are increasingly recognized as important in improving mental well-being. However, electroencephalography (EEG)-based neurofeedback systems supporting these practices typically fail to generalize to unseen subjects. This study investigates the application of both spatial and spectral alignment to EEG to improve the classification of meditation and rest states for new subjects without any model retraining. *Approach*. Two unsupervised domain adaptation techniques are employed to reduce differences between subjects in their EEG recordings. The first, Riemannian Space Data Alignment (RSDA), adjusts and brings together patterns of brain activity across electrodes (spatial domain). The second, Convolutional Monge Mapping Normalization (CMMN), aligns the distribution of brain rhythms across frequencies (spectral domain). Each method is evaluated separately, in combination, and in interaction with z-score normalization. Classification between meditation and rest is performed on the aligned time series using EEGNet, a compact convolutional neural network architecture, with leave-one-subject-out (LOSO) cross-validation to assess generalization across subjects. All experiments are based on a publicly available dataset of meditation EEG recordings from 53 subjects, including both novice and expert meditators. *Main results*. The combined RSDA+CMMN approach significantly improved LOSO classification accuracy (66.6%) compared to non-aligned (55.7%) and z-score normalized (59.6%) baselines, even though it did not improve overall harmonization. Spectral analysis identified consistent classification contributions from the Theta (4–8 Hz), Alpha (8–14 Hz), and Beta (14–30 Hz) bands, while spatial analysis highlighted Frontopolar and Temporal regions as critical for distinguishing the mental states of meditation and rest. *Significance*. This work is the first to explore both spatial and spectral alignment in subject-independent meditation decoding for improved cross-subject generalization. Aligning EEG time series without retraining provides a practical solution for real-time neurofeedback, thereby reducing subject variability and paving the way toward calibration-free neurotechnology that supports mental well-being.

© 2025 IOP Publishing Ltd. All rights, including for text and data mining, AI training, and similar technologies, are reserved.

1. Introduction

In contemporary society, the rapid pace of life has led to widespread stress, with anxiety becoming a prevalent condition [1]. To manage these challenges, meditation and mindfulness practices have been suggested as effective strategies for reducing stress and improving psychological well-being [2]. However, beginners often face difficulties in starting and maintaining a meditation practice [3]. Thus, developing effective, scientifically validated techniques to support novice practitioners would be highly beneficial. Neurofeedback offers real-time feedback on neural activity using electroencephalography (EEG) to help users monitor and modulate brain states.

In this context, accurate decoding and distinguishing between meditative and resting states is essential. To achieve this, researchers have utilized machine learning models combined with advanced feature engineering techniques to classify different cognitive states with greater precision [4, 5]. Especially, deep neural networks (DNNs) have demonstrated promising performance across various brain–computer interface (BCI) applications [6–8]. A key advantage of DNNs lies in their ability to autonomously extract subtle and previously overlooked features from EEG time series, thereby improving classification robustness. However, there remains a notable gap in the literature regarding the application of these methodologies for decoding mental states such as meditation and rest [9–11].

One of the main challenges in achieving robust classification is the high subject variability in EEG data. Subject variability can be described as the distribution shifts of the characteristics of the EEG time series obtained from different participants and is attributed to differences in brain anatomy, functionality, personality, and cognitive abilities among individuals [12]. Also, the non-stationarity of EEG signals [13], can lead to distribution shifts in EEG features. Together, these non-task-specific inconsistencies of the EEG signal render it impossible to train a single classification model that can robustly generalize and perform equally well on an unseen but independent and identically distributed dataset [12].

Given this variability, each individual subject can be regarded as a distinct domain, with their unique EEG characteristics introducing distribution shifts that pose significant challenges to model generalization. To address this, domain adaptation (DA) aims to mitigate distribution shifts by identifying and transferring shared attributes between domains, where each domain represents a different subject [12, 14, 15]. Accordingly, DA aims to minimize the discrepancy between the *source* domain, which consists of training data, and the *target* domain, representing the EEG data of an unseen test subject. Further, to avoid the need for extensive calibration, DA methods are typically designed to leverage target domain data in an unsupervised manner, minimizing the need for retraining of the model as much as possible.

To achieve DA in EEG decoding, various approaches focus on aligning the distributions of EEG time series, often leveraging geometric techniques. One common strategy is to use Euclidean geometry, where the Euclidean mean covariance matrix of each subject captures non-task-related information, facilitating the creation of domain-invariant representations [12, 16, 17]. Similarly, leveraging each subject's Riemannian Space Mean Covariance Matrix (RSMCM) enhances the performance of subject-agnostic models across various applications [18], including EEG-based meditation decoding [9]. Riemannian Procrustes Analysis (RPA) [19] goes one step further and includes two additional geometric operations of stretching and rotation. However, RPA is limited in its ability to generalize across multiple domains for transfer learning, and therefore, when more than one domain is involved or no directly aligned number of source and target domains are involved, RPA tends to fail, as it cannot effectively handle these complexities [20]. Some methodologies focus on developing subject-independent models, either overlooking subject variability challenges or utilizing ensemble learning to delineate in different domain subgroups [15]. While ensemble methods improve generalization, they often require additional computational resources and careful hyperparameter tuning, rendering their scalability and deployment more challenging in real-time applications.

This study addresses the challenge of subject variability in EEG time series analysis for decoding meditative vs rest states by investigating three DA methods including: spatial alignment, spectral alignment, and a combination of both on the EEG time series. Spatial alignment leverages the domain-wise RSMCM, which is hypothesized to capture non-task-related EEG activity responsible for subject variability. Spectral alignment is performed using the Convolutional Monge Mapping Normalization (CMMN) [21]. Aligning the spectral properties of EEG signals may be particularly effective, as previous studies showed power spectral density (PSD) to vary considerably among individuals [22]. In the present study, an alternative approach will be explored that integrates the advantages of spatial alignment through RSMCM with those of spectral alignment via CMMN. This approach ensures that PSDs from each domain are adjusted based on a barycenter computed from the source domains, while covariance matrices are aligned towards the identity matrix. This dual alignment strategy is expected to improve the generalizability of meditation-state classification models by aligning both the covariance structures (via RSDA)

and the mean PSDs (via CMMN), thereby enabling the extraction of uniform spectral features across subjects. Since these two methods act on complementary sources of variability, namely spatial and spectral, their combination is hypothesized to further enhance cross-subject generalization. Both alignment methods operate in an unsupervised manner, allowing for direct application to test data without requiring model retraining. Finally, the study evaluates the use of z-score normalization in both domain-wise and domain-wise-channel-wise forms as non-alignment baselines as well as in combination with different alignment approaches. This additional normalization step is motivated by reports stating that per-domain standardization can match or improve DA performance [23]. By systematically combining spatial and spectral adaptations, the study aims to determine whether addressing these complementary sources of variability results in additive benefits. Grounded in prior EEG variability research and DA theory, this approach is expected to enhance cross-subject generalization in EEG decoding. The inclusion of z-score normalization provides a simple statistical baseline, enabling a structured evaluation of the added value introduced by alignment-based methods.

The contributions of this work are the following:

- Aligning EEG time series is crucial for addressing the issue of subject variability. Both spatial and spectral alignment (RSDA+CMMN) help eliminate non-task-related information and reduce spectral distribution shifts between individuals. Notably, the use of spectral alignment, as well as the combined approach of spatial and spectral alignment, has not been previously applied in cross-subject meditation decoding.
- Providing a practical and efficient framework for real-time meditation neurofeedback. The proposed alignment methods operate in an unsupervised manner, allowing direct application to new subjects without requiring model retraining. This makes them well-suited for real-time BCI and neurofeedback applications designed to support meditation practice.

The remainder of the manuscript is structured as follows. Section 2 describes the proposed methods, dataset, and experimental procedure. Section 3 presents the results, followed by a discussion in section 4 and conclusions in section 5.

2. Methods

2.1. Problem and notation

Let $\mathcal{D}_{\mathcal{S}}$ and $\mathcal{D}_{\mathcal{T}}$ be two datasets, each consisting of domains (i.e. subjects), representing the $N_{\mathcal{S}}$ *source* domains and the $N_{\mathcal{T}}$ *target* domains, respectively:

$$\mathcal{D}_{\mathcal{S}} = \left\{ \mathcal{S}^{(d)} : d \in [N_{\mathcal{S}}] \right\} \tag{1}$$

$$\mathcal{D}_{\mathcal{T}} = \left\{ \mathcal{T}^{(d)} : d \in [N_{\mathcal{T}}] \right\}, \tag{2}$$

where each domain d in the *source* and *target* datasets is defined as follows:

$$\mathcal{S}^{(d)} = \left\{ \left(\mathbf{X}_i^{(d)}, \mathbf{y}_i^{(d)} \right) : i \in \left[T^{(d)} \right] \right\}, \mathcal{S}^{(d)} \in \mathcal{D}_{\mathcal{S}} \tag{3}$$

$$\mathcal{T}^{(d)} = \left\{ \left(\mathbf{X}_i^{(d)}, \mathbf{y}_i^{(d)} \right) : i \in \left[T^{(d)} \right] \right\}, \mathcal{T}^{(d)} \in \mathcal{D}_{\mathcal{T}}. \tag{4}$$

Each domain d consists of $T^{(d)}$ trials, where a trial refers to a single segment of recorded EEG data corresponding to a specific experimental condition. Each trial is represented as $\mathbf{X}_i^{(d)} \in \mathbb{R}^{C \times T}$, where i denotes the trial index, C is the number of EEG channels, and T is the number of time samples per trial. The corresponding class labels are given by one-hot-vectors $\mathbf{y}_i^{(d)} \in \mathbb{R}^L$, where L is the number of different conditions.

The problem investigated in this work is unsupervised DA in EEG. Specifically, the goal is to develop a procedure for aligning EEG data in an optimal way, ensuring that trials from each $\mathcal{S}^{(d)}$ and $\mathcal{T}^{(d)}$ are well-aligned. This alignment enables the decoding model to detect common attributes and generalize effectively to unseen domains that have undergone the same adaptation procedure.

Notation

For the remainder of the paper, the following notation will be used. The element wise power of n is represented by $\cdot^{\odot n}$, while $\odot$ is the element-wise multiplication between two matrices, and $|\cdot|$ is the element-wise magnitude of the complex vector. The operators $\mathfrak{F}(\cdot)$ and $\mathfrak{F}^*(\cdot)$ refer to the Fourier and inverse Fourier transforms, respectively. Lastly, the discrete convolution between two signals is represented by *.

2.2. EEG covariance matrix

The covariance matrix $\mathbf{\Sigma}_i^{(d)}$ of the EEG trial $\mathbf{X}_i^{(d)}$ is estimated as $\mathbf{\Sigma}_i^{(d)} = \mathbf{X}_i^{(d)} \mathbf{X}_i^{(d)\top} \in \mathbb{R}^{C \times C}$. This covariance matrix of size $C \times C$ is empirically known to be a symmetric positive definite (SPD) matrix.

2.3. Riemannian geometry

The SPD matrix of size $C \times C$ lies into the differentiable $\mathcal{P}(\Sigma)$ Riemannian manifold. If $\mathbf{\Sigma}_i^{(d)}$ and $\mathbf{\Sigma}_j^{(d)}$ are two covariance matrices with $i \neq j$ being two different trials from the same subject, then the *geodesic*, which is the Affine Invariant Riemannian distance metric [24], between those two matrices is defined as:

$$\delta\left(\mathbf{\Sigma}_i^{(d)}, \mathbf{\Sigma}_j^{(d)}\right) = \left(\sum_{h=1}^{C} \log^2 \lambda_h \right)^{\frac{1}{2}}, \tag{5}$$

with λ_h $(h \in [C])$ the real eigenvalues of $(\mathbf{\Sigma}_i^{(d)})^{-1}\mathbf{\Sigma}^{(d)}{}_j$.

Then, the RSMCM $\overline{\mathbf{\Sigma}}^{(d)}$ of a domain with $T^{(d)}$ trials is defined as the minimization matrix of the squared Riemannian distances, and is repeated for each domain, in both source and target sets as follows:

$$\overline{\mathbf{\Sigma}}^{(d)} = \arg\min_{\Sigma} \sum_{i=1}^{T^{(d)}} \delta^2 \left(\mathbf{\Sigma}, \mathbf{\Sigma}_i^{(d)}\right). \tag{6}$$

2.4. Riemannian space data alignment

Leveraging the characteristics of the SPD manifold, Riemannian alignment (RA)[24] was introduced as a method to re-center the covariance matrices of individual subjects around a reference covariance matrix, denoted as $\overline{\mathbf{\Sigma}}$. This process aims to suppress non-task-specific information [16, 24], thus enabling comparability among data from different subjects. Then, inspired by the EEG Euclidean space alignment [16], the Riemannian space data alignment (RSDA) was introduced as an alternative to align the EEG time-series [18]. If $\overline{\mathbf{\Sigma}}^{(d)}$ is the RSMCM of the EEG trials belonging to a domain d, the RSDA of each i-trial $\mathbf{X}^{(d)}{}_i$ for each domain is computed as

$$\hat{\mathbf{X}}_i^{(d)} = \overline{\mathbf{\Sigma}}^{(d)-\frac{1}{2}} \mathbf{X}_i^{(d)}, \tag{7}$$

where $\hat{\mathbf{X}}_i^{(d)}$ is the aligned ith trial of domain d. This procedure is again repeated for every domain.

2.5. CMMN

The multi-source DA with CMMN was introduced by [21] as a way to adapt and align the EEG PSD of all the domains via optimal transport to a Wasserstein barycenter estimated on the source domains. The optimal transport mapping between the barycenter and the PSD of each domain is computed, which acts as a temporal filter, shifting the spectral components of all the domains to resemble the spectral characteristics of the barycenter. This Wasserstein barycenter is independently computed for each channel in a multichannel setting.

The PSD $\hat{\mathbf{P}}^{(d)} \in \mathbb{R}^{C\times F}$ with F frequency components of all the trials $\mathbf{X}_i^{(d)} \in \mathbb{R}^{C\times T}$ of the preprocessed EEG can be approximated using Welch's method as $\hat{\mathbf{P}}^{(d)} = \frac{1}{T^{(d)}} \sum_{i=0}^{T^{(d)}} |\mathfrak{F}(\mathbf{X})_i^{(d)}|^{\odot 2}$. The barycenter $\overline{\mathbf{P}} \in \mathbb{R}^{C\times F}$ is then computed as:

$$\overline{\mathbf{P}} = \left(\frac{1}{N_{\mathcal{S}}} \sum_{s=1}^{N_{\mathcal{S}}} \hat{\mathbf{P}}^{(d)\odot\frac{1}{2}}\right)^{\odot 2}. \tag{8}$$

Once the barycenter is computed, then the optimal transport mapping between the trial $\mathbf{X}_i^{(d)}$ of any domain with domain-wise PSD $\hat{\mathbf{P}}^{(d)} \in \mathbb{R}^{C\times F}$ and the barycenter $\overline{\mathbf{P}} \in \mathbb{R}^{C\times F}$ is computed by first determining the domain-wise adjusted temporal filter $\mathbf{H}^{(d)} = \mathfrak{F}^* \left(\overline{\mathbf{P}}^{\odot\frac{1}{2}} \odot \hat{\mathbf{P}}^{(d)\odot\frac{-1}{2}}\right)$ followed by the convolutional operation

$$\mathcal{M}\left(\mathbf{X}_i^{(d)}\right) = \mathrm{Conv}\left(\mathbf{H}^{(d)}, \mathbf{X}_i^{(d)}\right) = \begin{bmatrix} \mathbf{h_1} * \mathbf{x}_1^{(d)} \\ \mathbf{h_2} * \mathbf{x}_2^{(d)} \\ \vdots \\ \mathbf{h_C} * \mathbf{x}_C^{(d)} \end{bmatrix}, \tag{9}$$

where $\mathbf{H}^{(d)} \in \mathbb{R}^{C\times T_f}$ represents the temporal filter as computed for each domain d, with T_f being the temporal size of the filter. Finally, $\mathcal{M}(\mathbf{X}_i^{(d)})$ represents the temporally aligned $\mathbf{X}_i^{(d)}$ trial of domain d, $\mathbf{h}_c$ represents the temporal filter for cth channel, and $\mathbf{x}_c$ represents the EEG of the cth channel.

Z-score normalization

Apicella *et al* (2023) [23] examined the impact of z-score normalization on EEG data across various DA techniques for emotion recognition and motor imagery decoding. They found that normalizing each domain's EEG individually improved DA performance and, in some cases, even outperformed DA methods. This study also evaluates z-score normalization as a baseline to assess whether alignment methods provide additional benefits. Each EEG value is standardized based on its time-series mean and standard deviation. Additionally, domain- and channel-specific normalization is considered, where normalization is applied separately to each channel within each domain. Hereafter, $Z^{(d)}$ denotes domain-specific normalization, while $Z_{\mathrm{ch}}^{(d)}$ refers to channel-specific normalization within each domain.

2.6. Architecture

EEGNet [6], a compact yet effective architecture for EEG decoding, is widely applied in BCI tasks, including meditation decoding [9]. Its efficiency stems from a minimal parameter count while maintaining strong performance. EEGNet consists of two convolutional blocks and a fully connected layer, leveraging temporal and depthwise convolutions, nonlinear activations, and average pooling to extract frequency-specific spatial features. EEG trials $\mathbf{X}^{(d)}i$ serve as inputs, producing class-wise scores $\hat{\mathbf{y}}^{(d)}i \in \mathbb{R}^L$, optimized against ground-truth labels $\mathbf{y}_i^{(d)} \in \mathbb{R}^L$ using cross-entropy loss.

2.7. Dataset

A publicly available dataset with meditation and mind wandering tasks was utilized: the *ExpertsNovices* [25]. A brief description of the dataset is provided in the following paragraph followed by the preprocessing pipeline is presented.

ExpertsNovices

EEG recordings from 58 healthy young adults (29 Experts and 29 Novices, with 5 subjects excluded due to incomplete data or bad data quality) were utilized and evaluated across two conditions: a rest period lasting 5 min, and a breath focus meditation session lasting a total of 10 min, with only the final 5 min considered for the analysis presented here. These data were obtained as part of a larger study, detailed in [25]. During the rest period, participants were instructed to keep their eyes closed, refrain from sleeping, minimize movement, and allow their thoughts to wander freely. In the meditation condition, participants followed the guidelines as outlined here: '*Sit in a comfortable posture that embodies dignity, keeping the spine straight and letting your shoulders drop. Close your eyes and allow your attention to gently align to the sensation of breathing. You can focus on the part of your body where you feel your breath most clearly (for example: nostrils, belly, chest…). Every time you notice that your mind has wandered off your breath, notice what it was that carried you away, and then gently bring your attention back to the sensations associated with your breath*' [25, 26]. Continuous EEG data were captured using a 19-electrode cap positioned according to the international $10-20$ system, along with two reference electrodes and one ground electrode. The EEG signals were sampled at 512 Hz. The mindful attention awareness scale (MAAS) [27] was completed by the participants before the recording sessions, in order to assess their ability to remain attentive and aware of the present moment. The average of the reported answers was then calculated, yielding an index ranging from 1 to 6, with higher values indicating higher mindfulness levels. All participants provided written informed consent, and the study design and consent forms were approved by the Social and Societal Ethics Committee (SMEC) of KU Leuven, in accordance with the Declaration of Helsinki (dossier no. G-2019 09 1747). Participants received 8 euros per hour and had their travel expenses covered.

Preprocessing

The EEG preprocessing was performed using Python with functions from the MNE and Braindecode libraries. The preprocessing pipeline applied to the raw EEG data included the following steps: (1) elimination of low-frequency and high-frequency noise using a band-pass filter with cut-off frequency $1-125$ Hz , (2) removal of the 50 Hz component using a notch filter (5th-order Butterworth filter with a 2 Hz bandwidth), (3) identification and removal of flat or noisy channels followed by reconstruction using spherical interpolation, (4) re-referencing the data to a common average reference, (5) performing independent component analysis to automatically discard noisy components related to muscle activity, eye movement, heart artifacts, or channel noise using the `iclabel` algorithm, and (6) downsampling the data from 512 Hz to 256 Hz. No additional correction or rejection of trials based on quality criteria was applied.

Regarding segmentation, the continuous EEG recordings in the dataset for each of the two conditions under study were divided into non-overlapping segments of duration 1 s after pre-processing. These segments were utilized as trials, resulting in matrices of size 19×256 for each time-segment. Furthermore, the number of trials for each condition varied, with counts of around 300 segments for each subject ($n = 600$ samples in total for both conditions).

RSDA and CMMN computation

To apply RSDA to each domain, the Riemannian mean for each domain was computed by estimating all trial-wise matrices from each EEG trial of size 19×256, without considering any class information. Similarly, for the computation of the barycenter, the domain-wise PSD was obtained by calculating the PSD of each trial for each domain and then averaging them, again without considering any class information. The Welch transform window was set to 256, equal to the trial duration, with no overlap. For both RSDA and CMMN, the entire 15 min of recording were used without any class information. After computing the Riemannian mean and the barycenter, the first 5 min of the meditation condition were discarded to obtain a balanced dataset.

2.8. Experiments

A series of experiments were conducted to assess whether the proposed methodology can improve meditation decoding.

Group separation

Previous studies have explored distribution alignment across one-to-one domains using RSDA on covariance matrices or Euclidean Data Alignment on EEG data [12, 16, 24]. The first experiment (section 3.1) evaluates the proposed methodology's effectiveness in reducing individual differences within the *ExpertsNovices* dataset, consisting of 25 Experts and 28 Novices, each with approximately 300 samples per condition. A lower classification accuracy indicates better domain alignment, as it suggests reduced inter-domain differences, particularly between these two groups.

Classification of meditation and rest states

To evaluate the proposed methodology, a second experiment (section 3.2) assessed classification accuracy for meditation vs rest. Another experiment (section 3.4) examined the impact of alignment,

normalization techniques, and spectral components learned by the model. EEG signals were band-pass filtered into θ (4–8 Hz), α (8–14 Hz), β (14–30 Hz), low γ (30–50 Hz), and high γ (50–100 Hz), followed by classification for each frequency band, normalization, and alignment approach.

Impact of EEG frequency bands and channel removal on meditation vs rest classification

For stress regulation applications, compact, wearable EEG caps are essential. To assess adaptability for home-based setups (section 3.5), channel contributions were evaluated. Three experiments analyzed the impact of different EEG regions (figure 5(a)) on classification: (1) using only Frontopolar-Temporal electrodes (blue, 8 channels), (2) excluding these while retaining Central-Parietal-Occipital electrodes (purple/green, 11 channels), and (3) further reducing to only Parietal-Occipital electrodes (green, 8 channels).

Mindfulness level impact on classification accuracy

To examine whether meditation decoding accuracy was associated with individual subject characteristics, Pearson correlations were computed between the leave-one-subject-out (LOSO) classification accuracy and the MAAS score for each individual, using each method.

2.9. Experimental details

This subsection offers a detailed summary of the implemented methods and the experiments carried out to assess the effectiveness of the proposed methods. All computations were performed using Python.

Evaluation settings

Following [9], this study employed a LOSO evaluation, a many-to-one transfer learning approach. Each fold designated one subject as the test set (target domain), with 20% of the remaining subjects randomly assigned for validation and 80% for training (source domains). The alignment methods included RSDA, CMMN, RSDA+CMMN, and their combinations with two types of z-score normalization (figure 1). These alignments were applied to preprocessed EEG data before training EEGNet. In CMMN, the barycenter was learned exclusively from the training set, while RSDA, being subject-specific, did not require this constraint. EEGNet was re-initialized from scratch for each fold to prevent any data leakage across folds. Classification accuracy served as the evaluation metric.

EEGNet training hyperparameters

All the experiments conducted and presented in this work complied with the identical training procedure and specifications outlined in [9]. For training

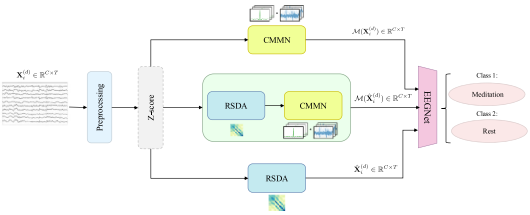


Figure 1. Overview of the alignment methodology. The flow diagram illustrates the investigated domain adaptation techniques: Riemannian Space Data Alignment (RSDA), Convolutional Monge Mapping Normalization (CMMN), and their sequential application (RSDA → CMMN). Each method is applied with or without prior z-score normalization ($Z^{(d)}$, $Z^{(d)}_{\text{ch}}$), resulting in twelve alignment pipelines. The aligned EEG signals are then classified into meditation and mind-wandering states using EEGNet.

EEGNet, the batch size was set at 64, the dropout rate was 0.3 and 120 epochs were used. The Adam optimizer was used with 0.01 weight decay, without hyperparameter tuning. The learning rate was initially set to $lr = 0.01$ and then decreased to $lr = 0.001$ and $lr = 0.0001$ in epochs 10 and 75, respectively. All models were trained on NVIDIA GeForce RTX 2080 and NVIDIA GeForce RTX 3070 GPUs, with CUDA 11.8, using the `PyTorch` framework[5] (version 1.10.0).

Statistical tests

Wilcoxon signed-rank tests were adopted to explore significant differences between performance. Multiple comparison corrections were applied using the Holm–Bonferroni (HB) method to adjust p-values, ensuring control over the family-wise error rate [28]. A significance threshold of $p < 0.05$ was adopted to determine statistical significance.

3. Results

3.1. Group separation

To evaluate whether the alignment techniques reduced distributional differences between domains, an experiment was conducted assessing group separation (novices vs experts) for each condition independently (see table 1). Specifically, in the absence of alignment or when using CMMN, group separation exceeded chance-level performance, resulting in average accuracy scores of 60.1% and 58.5%, respectively, when analyzing data from the meditative state. In contrast, when applying z-score normalization or any of the remaining alignment techniques in the meditative state, group separation decreased to chance-level performance, falling below the acceptable chance threshold of 58% for a sample size of $n = 300$ [29]. When analyzing the resting state data, the results were consistently below the chance level,

[5] https://pytorch.org/.

Table 1. Group separation (novices vs experts) LOSO accuracy results for each condition.

Alignment method	Resting state	Meditative state
No-Alignment	52.5%	60.1%
$Z^{(d)}$	49.9%	54.8%
$Z^{(d)}_{\text{ch}}$	58.4%	51.%
RSDA	48.2%	52.9%
CMMN	55.%	58.5%
RSDA+CMMN	51.1%	55.9%

indicating that this state is already well-aligned across subjects. Overall, the results suggest that the alignment techniques are successful in bringing the different domains closer together, particularly in the Meditative state, which is expected to show more differences between novices and experts.

3.2. Classification of meditation and rest states

The LOSO accuracy results for classifying rest vs meditation (figure 2) show that without alignment, performance was only slightly above chance. However, applying alignment techniques significantly improved accuracy.

No prior normalization

The proposed approach, RSDA+CMMN, achieved the highest average accuracy of $66.6 \pm 22.3\%$, significantly outperforming the NoAlignment baseline ($+10.9\%$, $p = 0.004$) and the CMMN condition ($+8.2\%$, $p = 0.01$). However, the difference compared with RSDA alone was not statistically significant ($+2.8\%$, $p = 0.6$), suggesting that most of the improvement arises from the spatial alignment component. Despite higher mean accuracy, RSDA+CMMN also exhibited increased inter-subject variability, indicating that its benefits were not consistent across participants. When examined individually, RSDA enhanced average accuracy to $63.9 \pm 20.3\%$, with half of the subjects exceeding the NoAlignment baseline (55.7%), although some participants performed below 30%. CMMN, focusing on spectral alignment, yielded a moderate improvement to $58.4 \pm 14.6\%$, with at least half of the subjects performing above 56.1%. Overall, these results confirm that combining spatial and spectral alignment maximizes performance on average, but the increased variability highlights the need for further robustness analysis. Notably, spectral alignment preceding spatial alignment was not tested, as this order would disrupt spatial structure.

Per domain Z-score normalization

Domain-level normalization ($Z^{(d)}$) provided only limited benefits overall. The proposed approach, RSDA+CMMN, remained significantly more accurate than the NoAlignment baseline ($+8.6\%$, $p = 0.03$)

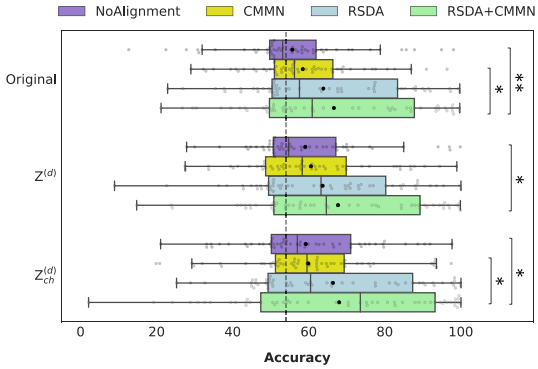


Figure 2. LOSO accuracy for meditation vs rest Classification. The black dashed line marks chance-level performance for $n = 600$ test samples (54% for $n > 500$ [29]). The black dot represents average accuracy, and transparent dots indicate individual subject performances. Three cases were analyzed: (1) original (no z-score normalization), (2) $Z^{(d)}$ (domain-wise z-score), and (3) $Z^{(d)}$ ch (channel- and domain-wise z-score). RSDA+CMMN generally achieved higher accuracy than other methods (Original: RSDA $+2.8\%$, $p = 0.6$, $Z^{(d)}$: CMMN $+7,1\%$, $p = 0.085$, RSDA $+4.1\%$, $p = 0.065$, $Z^{(d)}$ ch: RSDA $+1.6\%$, $p = 0.7$). Statistical significance (Wilcoxon signed-rank tests, HB corrected) is marked as $(*)$ $p \leqslant 0.05$ and $(**)$ $p \leqslant 0.01$.

with an average accuracy of 68%, indicating that alignment remained the main driver of performance gains. However, when normalization was applied, its contribution to accuracy was modest and did not consistently improve results. In particular, the advantage of RSDA+CMMN over CMMN alone was reduced ($+7.1\%$, $p = 0.085$) and no longer statistically significant. Similarly, the difference between RSDA and RSDA+CMMN was small ($+3.2\%$, $p = 0.065$), with median accuracy remaining nearly unchanged (62.3% vs 63%). When tested independently, normalization led to slight gains of $+3.3\%$ without alignment, when compared with no-zscore normalization, and $+2.3\%$ when combined with CMMN. These results suggest that while normalization may offer minor improvements, its effect is not statistically robust and has limited practical impact.

Per channel and subject Z-score normalization

Channel-wise normalization ($Z^{(d)}_{\text{ch}}$) yielded results comparable to domain-level normalization ($Z^{(d)}$), offering no additional benefit. The combined approach, RSDA+CMMN, continued to outperform both NoAlignment ($+8.8\%$, $p = 0.045$) and CMMN ($+8.1\%$, $p = 0.045$), demonstrating that the gains were primarily driven by the alignment strategy rather than the normalization scheme. Although the performance gap between RSDA+CMMN and RSDA further narrowed ($+1.6\%$, $p = 0.72$), the median accuracy of RSDA+CMMN increased slightly to 72%. Overall, normalizing EEG channels prior to

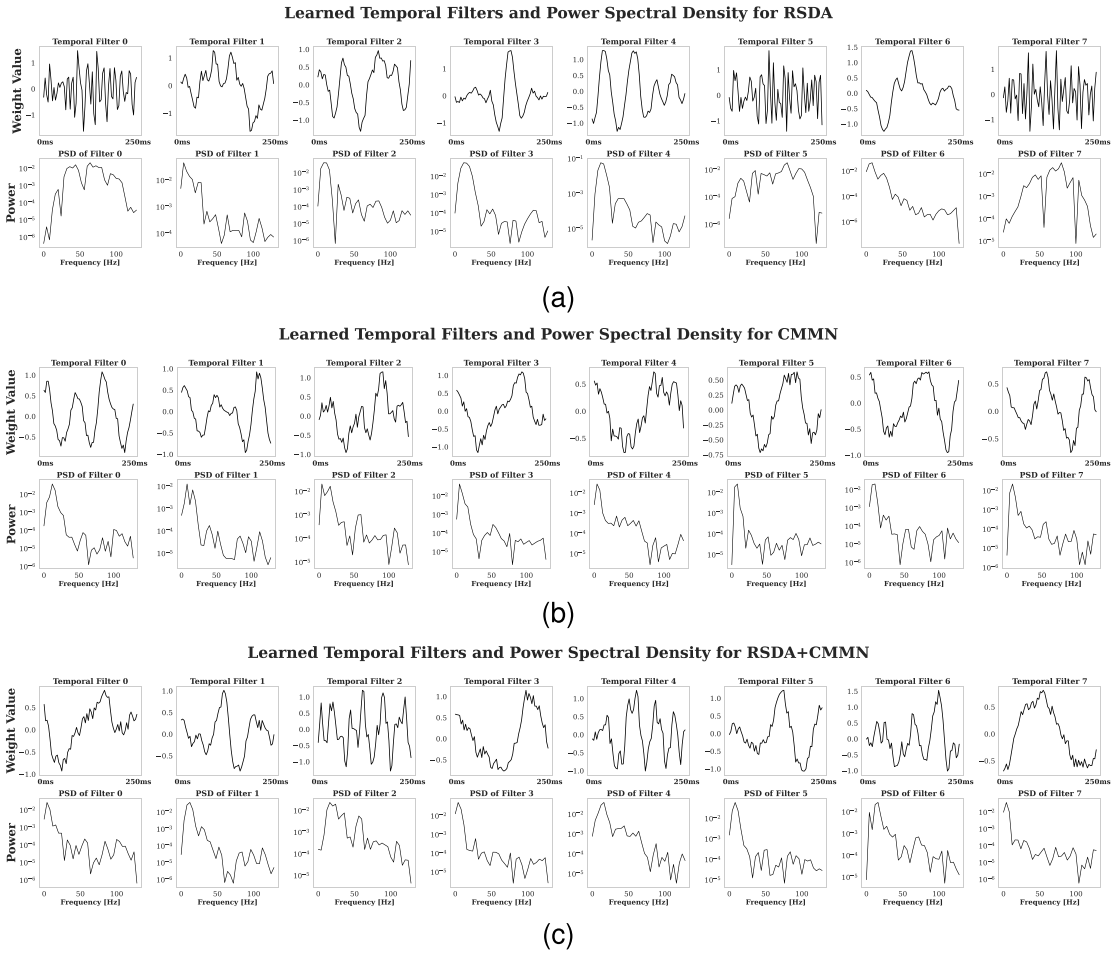


Figure 3. Learned Temporal Filter Weights and PSDs from EEGNet's First Convolutional Layer for Each EEG Alignment. (a) With RSDA EEGs, filters captured information across all frequency bands, from low (filters 1, 3, 6) to high (filters 0, 5, 7). (b) CMMN-aligned EEGs primarily emphasized lower frequencies. (c) RSDA+CMMN EEGs incorporated both lower and slightly higher frequency components (e.g. filter 2).

alignment did not yield statistically or practically meaningful improvements.

3.3. Learned spectral components

The spectral filters learned by EEGNet were examined to assess the impact of alignment methods (figure 3). RSDA-aligned EEGs resulted in filters spanning a broad frequency range, with lower frequencies (4–30 Hz) and higher frequencies (50–100 Hz) contributing to classification. This suggests RSDA reduces the dominance of low-frequency components, enhancing multi-scale feature extraction. In contrast, CMMN-aligned EEGs produced filters predominantly within lower frequencies (4–25 Hz), indicating a shift toward slower oscillations. When RSDA and CMMN were combined, the learned filters reflected a more balanced frequency representation, retaining both low- and high-frequency information. This suggests RSDA preserves high-frequency details, while CMMN suppresses them, with their combination yielding a more comprehensive spectral distribution.

3.4. Impact of EEG frequency bands

The classification results for each case are shown in figure 4. In most cases, a consistent trend was observed across bands, where the combination of RSDA+CMMN yielded the highest average classification accuracy. However, the degree of improvement varied by frequency band, suggesting that certain oscillatory components contribute more significantly to distinguishing rest from meditation.

Theta band

RSDA+CMMN achieved the highest overall accuracy, peaking at $66.4(\pm16.6)\%$ for $Z^{(d)}_{\text{ch}}$, without significant differences when no z-score normalization was applied (65.2%) or when $Z^{(d)}$ was applied (64.9%) . This performance was significantly higher than that of NoAlignment (Original: +8.6%, $p = 1.5 \times 10^{-3}$, $Z^{(d)}$: +6.1%, $p = 7 \times 10^{-3}$, $Z^{(d)}_{\text{ch}}$: +7.6%, $p = 4 \times 10^{-4}$), RSDA alone (+9.2%, $p = 3.4 \times 10^{-4}$, $Z^{(d)}$: +14.5%, $p = 3 \times 10^{-6}$, $Z^{(d)}_{\text{ch}}$: +10.2%, $p = 8 \times 10^{-6}$), and CMMN alone (+5.4%, $p = 0.016$, $Z^{(d)}$: 4.4%, $p = 0.01$, $Z^{(d)}_{\text{ch}}$: +6.8%, $p = 8 \times 10^{-4}$), confirming

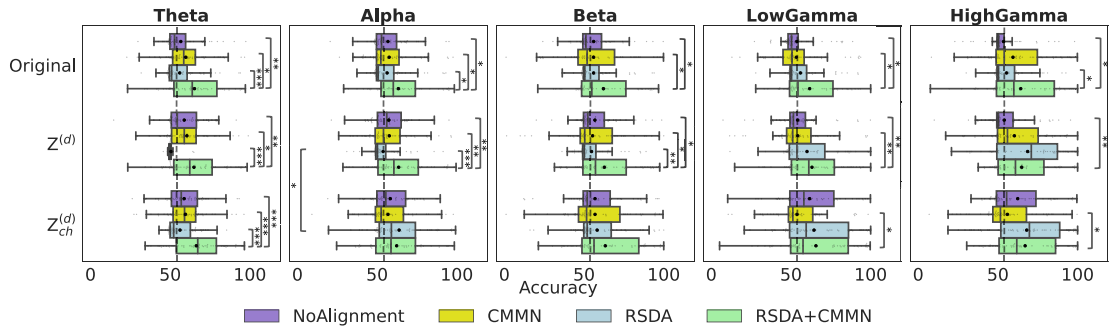


Figure 4. LOSO accuracy across frequency bands for rest vs meditation. The black dashed line indicates chance level performance. The black dot represents average accuracy, and gray dots show individual subject performances. Classification was conducted across five bands: $\theta = [4, 8)$ Hz, $\alpha = [8, 14]$ Hz, $\beta = (14, 30]$ Hz, low $\gamma = (30, 50]$ Hz, and high $\gamma = (50, 100]$ Hz, using three preprocessing approaches: (1) Original (no z-score normalization), (2) $Z^{(d)}$ (domain-wise z-score), and (3) $Z^{(d)}$ch (channel- and domain-wise z-score). RSDA+CMMN consistently outperformed other techniques, especially in θ and α bands. In the α band with $Z^{(d)}$ch, RSDA alone performed comparably to RSDA+CMMN. Applying $Z^{(d)}$ before RSDA+CMMN improved accuracy. Statistical significance (Wilcoxon signed-rank tests, HB corrected) is marked as (*) $p \leqslant 0.05$, (**) $p \leqslant 0.01$, (***) $p \leqslant 0.001$.

the strong complementary effect of spatial and spectral alignment. In contrast, NoAlignment and CMMN yielded only moderate accuracies (56%–60.5%), while RSDA alone performed the worst, particularly under domain-level normalization ($Z^{(d)}$), where accuracy dropped to 50.4%. These findings underscore the critical importance of the theta band in accurate meditation-state decoding.

Alpha band

RSDA+CMMN, consistently outperformed all other methods, achieving accuracies of $63.3 \pm 18.0\%$ and $63.5 \pm 18.2\%$ for raw and per-subject ($Z^{(d)}$) normalized data, respectively. These results were significantly higher than those of NoAlignment (+6.6%, $p = 0.010$ and +6.2%, $p = 0.001$), RSDA alone (+7.1, $p = 0.010$ and +9.8%, $p = 2.5 \times 10^{-4}$), and CMMN alone (+5.8%, $p = 0.010$ and +5.9%, $p = 0.004$). However, under channel-wise normalization ($Z^{(d)}_{\text{ch}}$), RSDA+CMMN provided no further advantage over the baselines (vs No-Alignment: +4%, $p = 0.056$; vs RSDA: -1.5%, $p = 0.750$; vs CMMN: +5.4%, $p = 0.056$). Both NoAlignment and CMMN achieved similar accuracies (56%–58%), while RSDA alone exhibited high variability (53.8%–63.8%). These findings suggest that the alpha band contains sufficient discriminative information for meditation-state classification, particularly when amplitude coupling is reduced through channel-wise normalization.

Beta band

RSDA+CMMN achieved the highest accuracy ($63.3 \pm 20.8\%$ with $Z^{(d)}_{\text{ch}}$ normalization), although the improvements were not statistically significant when compared with NoAlignment (+6.5%, $p = 0.148$), RSDA alone (+5.2%, $p = 0.148$), or CMMN alone (+6.5%, $p = 0.148$). Overall, RSDA+CMMN consistently led in overall best performance when no prior normalization (Original) or per domain normalization ($Z^{(d)}$) was applied when compared to NoAlignment baseline (Original: +6.1%, $p = 0.04$, $Z^{(d)}$: +5.9%, $p = 0.02$) or CMMN (Original: +6.1%, $p = 0.027$, $Z^{(d)}$: +7.3%, $p = 0.03$). Compared to RSDA, RSDA+CMMN showed better but non-significant performance when no prior normalization was applied (+6.1%, $p = 0.09$), and a significant improvement once $Z^{(d)}$ was applied (+8%, $p = 0.008$). Both NoAlignment and CMMN yielded moderate accuracies (55%–57%), while RSDA alone performed slightly lower (54.7%–58.2%). Overall, these results suggest that spatial and spectral alignment provide only marginal advantages within the beta band, yet they emphasize the importance of aligning beta band components for effective classification.

Low and high gamma band

In the gamma range, performance varied across subbands. The combined approach, RSDA+CMMN, achieved the highest accuracy in the low gamma band ($65.7 \pm 24.0\%$ with $Z^{(d)}$ normalization), significantly outperforming NoAlignment (+8%, $p = 0.010$) and CMMN alone (+8.3%, $p = 0.009$), while showing no significant difference compared with RSDA alone (+5.8%, $p = 0.241$). In contrast, RSDA alone performed best in the high gamma band ($68.7 \pm 22.0\%$ with $Z^{(d)}$ and $68.1 \pm 23.2\%$ with $Z^{(d)}_{\text{ch}}$). Both NoAlignment and CMMN produced lower accuracies (53%–62%). Despite high classification performance, gamma band results require caution due to sensitivity to muscle artifacts [30].

3.5. Effects of channel removal

Figure 5(b) shows classification accuracy across different EEG groupings and preprocessing methods. The Frontopolar-Temporal grouping yielded the

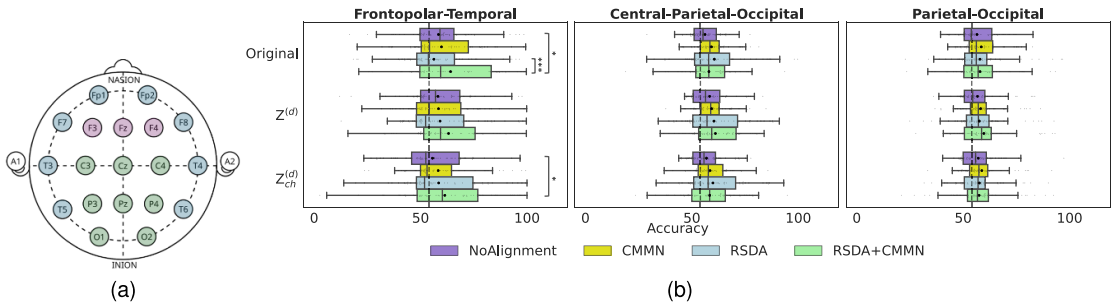


Figure 5. LOSO accuracy for meditation vs rest across EEG channel groupings. The black dashed line indicates chance-level performance. The black dot represents average accuracy, and gray dots show individual subject performances. Three channel groupings were analyzed: Frontal-Temporal (blue), Central-Parietal-Occipital (pink/green), and Parietal-Occipital (green). Each grouping was evaluated using: (1) Original (no z-score normalization), (2) $Z^{(d)}$ (domain-wise z-score), and (3) $Z^{(d)}_{\text{ch}}$ (channel- and domain-wise z-score). The Frontopolar-Temporal grouping showed slight performance improvements across preprocessing methods, with RSDA+CMMN achieving accuracy comparable to the full 19-channel EEG. The Central-Parietal-Occipital grouping had lower accuracy and variability, with RSDA+CMMN performing similarly to CMMN or RSDA alone. The Parietal-Occipital grouping showed a modest accuracy increase with RSDA+CMMN and a tighter distribution of performances. These findings highlight the importance of Frontopolar-Temporal channels in classification, particularly with RSDA+CMMN. Statistical significance (Wilcoxon signed-rank tests, HB corrected) is marked as (*) $p \leqslant 0.05$ and (***) $p \leqslant 0.001$.

highest overall accuracy, particularly for the combined approach RSDA+CMMN ($63.8 \pm 20.3\%$), which significantly outperformed NoAlignment ($+5.7\%$, $p = 0.02$) and RSDA alone ($+7.8\%$, $p = 4 \times 10^{-4}$), while showing better, but no significant, difference relative to CMMN ($+4.3\%$, $p = 0.051$). Reducing the montage to 11 electrodes (Central-Parietal-Occipital configuration) resulted in a slight decrease in performance compared with the full 19-channel configuration, suggesting that whole-scalp EEG provides complementary spatial information that is beneficial for classification. For non-aligned EEG (NoAlignment), LOSO accuracy remained stable at $55.5 \pm 8.0\%$, with reduced variability across participants. When Frontopolar-Temporal electrodes were removed (Central-Parietal-Occipital configuration), RSDA accuracy declined from $63.0 \pm 2.0\%$ to $59.5 \pm 16.0\%$, highlighting their importance for spatial whitening. Excluding all frontal electrodes further decreased accuracy for both RSDA ($57.0 \pm 14.0\%$) and NoAlignment ($56.4 \pm 9.0\%$) conditions. For CMMN, performance on the 11-channel EEG remained comparable to that of the full montage ($57.1 \pm 15.0\%$ vs $57.2 \pm 17.0\%$), indicating robustness to moderate channel reduction. In contrast, accuracy in the 8-channel Parietal-Occipital setup slightly increased ($58.4 \pm 9.0\%$), whereas RSDA+CMMN performance declined for both 11- and 8-channel sets ($58.0 \pm 15.0\%$), showing limited benefit when channels were removed (vs No-Alignment: $+1.5\%$, $p = 0.69$; vs RSDA: $+0.1\%$, $p = 0.88$; vs CMMN: $+0.5\%$, $p = 0.85$). Z-score normalization had no additional effect on accuracy (vs NoAlignment: Original: $p = 0.045$; vs RSDA: $p = 0.72$; vs CMMN: $p = 0.045$).

These results confirm that Frontopolar-Temporal channels are crucial for distinguishing rest from meditation. Their removal reduces performance, though RSDA and CMMN still enhance decoding even with fewer channels.

3.6. Mindfulness level impact on classification accuracy

In all analyses, no significant associations between the average MAAS score and the LOSO classification accuracy were observed (all $p > .05$). Effect sizes were small, with correlation coefficients ranging from $r = 0.05$ to $r = 0.17$. Scatterplots (figure 6) illustrate weak positive trends in each case; however, none of these trends reached statistical significance. These findings indicate that variability in meditation decoding performance was largely independent of the mindfulness level as reported by MAAS.

4. Discussion

4.1. Group separation

To assess whether alignment methods reduce inter-subject variability, we tested if the two groups (novices and experts) remained distinguishable post-alignment. Novice meditators typically experience higher cognitive load and more rest, leading to differences in spectral characteristics compared to experts [3, 25]. Results showed that without alignment, group discrimination was higher, whereas alignment techniques reduced it to below chance levels. This supports the hypothesis that spatial and spectral alignment bring EEG distributions closer together by suppressing non-task-related activity. While some subjects still performed at chance level or showed opposite trends, these individuals were evenly distributed across both groups, indicating that alignment does not disproportionately affect one group over the other.

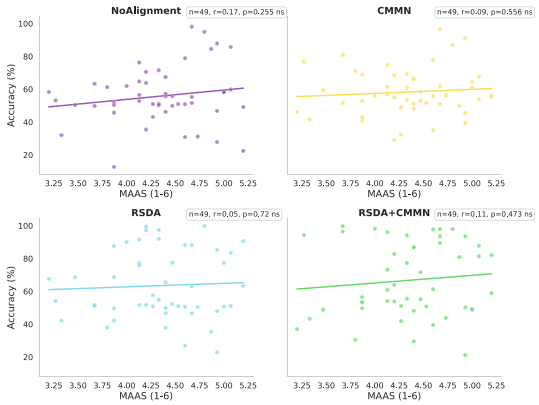


Figure 6. Statistical relationship between LOSO classification accuracy and MAAS scores across alignment conditions. Each subplot is color-coded according to the alignment method. Scatter points represent individual subjects, with LOSO accuracy plotted against their corresponding MAAS score. The regression line is shown in each plot. No statistically significant correlations were observed between LOSO accuracy and MAAS across alignment methods. Here, *n* denotes the number of subjects with available MAAS data, *r* is the Pearson correlation coefficient, and 'ns' indicates a non-significant *p*-value.

4.2. Effects of spatial and spectral alignment across EEG frequency bands

For cross-subject decoding of the meditative state, spatial and spectral alignment improved classification performance compared to non-aligned models. RSDA and RSDA+CMMN provided the greatest benefits, even within individual bands, though with high inter-subject variability [9]. RSDA reduced signal power by removing inter-channel correlations, potentially affecting channels previously critical for classification. CMMN, which shifts the PSD toward higher power frequencies, was less influenced by *z*-score normalization but suppressed higher spectral components, impacting cognitive state classification.

Key frequency bands (θ, α) are essential for decoding meditation, while β relates to stress and overthinking [31]. RSDA+CMMN consistently improved classification, particularly in θ, α, and β bands. $Z_{\text{ch}}^{(d)}$ normalization notably enhanced accuracy in the α band, possibly by preserving oscillatory coupling while altering absolute power variance. This suggests that the α band alone may contain sufficient meditation-related information.

Interestingly, RSDA alone captured key features in low and high γ bands, highlighting its ability to preserve meaningful spectral content. Given that electromyographic activity can amplify EEG γ signals [30], excluding γ may be advisable in meditation studies focused solely on brain activity. CMMN showed limitations when applied to broadband EEG, suggesting it is best suited for narrower frequency ranges. Additionally, low-frequency δ rhythms (1–4 Hz) may also play a role in attentional engagement during meditation [32].

4.3. General discussion

This work assumes participants understood and followed task instructions, though this may not always be the case. The results show that as performance improves, variability increases, sometimes leading to opposite outcomes among subjects. This suggests that the ground truth may not always align with the assigned labels. Potential explanations include rest episodes during meditation [33] and expert meditators' ability to transition quickly between rest and attentive states [34]. While spatio-temporal alignment may capture condition distributions and help the model learn key features, results were inconsistent across individuals, likely due to uncertainty in ground-truth labeling.

Studies have shown that meditation-related activity is distributed across the EEG scalp [35]. Three additional experiments examined brain regions contributing to task discrimination, finding significant contributions from the frontopolar and temporal regions. This aligns with previous studies showing frontopolar activation in meditation [36] and θ band synchronization in parietal regions during meditation [37]. Although removing these channels decreased performance, spatial and spectral alignment still improved meditation decoding, suggesting relevant information remains in these regions. The performance drop could also be linked to the loss of inter-channel information through RSDA, underscoring the potential importance of EEG connectivity in distinguishing mental states.

Applications to anxiety and stress

Anxiety and acute stress are associated with shifts in α, θ, and β activity and engagement of frontopolar and temporal regions [38]. In line with this, consistent contributions from θ (4–8 Hz), α (8–14 Hz), and β (14–30 Hz) are observed, with main effects over frontopolar/temporal regions. These

correspondences suggest that the features supporting meditation decoding are also informative for stress regulation. Within this context, the proposed unsupervised DA alignment, which aligns the spatial and temporal EEG information (CMMN+RSDA), yields subject-independent decoders operating on θ, α, and β features, incorporating frontopolar-temporal information and thereby enabling stress applications without requiring user-specific retraining. During mindfulness practice, the same signals can index session quality by detecting transitions into non-meditative or high-arousal patterns and prompting brief regulation (e.g. paced breathing, attentional refocusing). In everyday settings, sensitivity in the β range can serve as a marker of arousal [31]. Longitudinally, decoder-derived indices (e.g. time spent in a meditative state) can be paired with brief symptom scales to track anxiety/stress alongside practice quality. To increase brain specificity, γ can be excluded given susceptibility muscle activity contamination [30]. Finally, the robustness of frontopolar and temporal contributions, together with acceptable performance on smaller montages, indicates that practical sensor placements can support real-world stress applications without calibration.

Extension of spatial and spectral alignment to other applications

The combination of RSDA and CMMN is expected to be especially effective in applications where spectral components provide critical information for mental state decoding. In meditation, for example, it has already been shown that the frequency information is important in characterizing meditation and distinguishing between different states, as supported and shown by various studies [4, 5, 9, 25] and therefore individual variability in spectral properties can strongly influence decoding, making frequency alignment particularly important. Another application where spatial and spectral alignment could also provide benefits is mental workload classification for passive BCIs, as described in [39, 40], where frequency band information was found to be a statistically significant factor for distinguishing workload states, and an interaction was observed between workload level and electrode location.

4.4. Limitations and future directions

While spatial and spectral alignment improve cross-subject meditation decoding, limitations remain. Some subjects exhibited opposite performance trends, suggesting that the model's distinguishing features may not be universal, potentially due to individual physiological and anatomical differences. Practically, this implies that alignment-based approaches may still require some degree of subject-specific calibration in real-world or clinical settings, as inter-individual variability can limit generalization. One solution is Domain Selection, choosing subjects with similar attributes to improve performance [41]. Additionally, the lack of absolute quantification in meditation complicates task verification, posing challenges for reproducibility and standardization where objective validation metrics are essential. Current alignment methods are tested only for offline decoding, but future work should assess their practicality for online experiments, where real-time adaptation, robustness to signal noise, and computational efficiency will be critical. Finally, EEG connectivity should be considered, as it may involve information lost in the proposed methods. In this regard, approaches such as the Spatio-Temporal Monge Mapping technique [42], which incorporates cross-channel spectral information when computing the barycenter, represent a valuable extension that models inter-channel associations.

Another limitation is that the benefits of combining spatial and spectral alignment may not transfer equally across all paradigms. For instance, in motor imagery tasks, brain activity is primarily driven by Event-Related Synchronization emerging from averaged time-frequency representations, making frequency information secondary. Similarly, in event-related potentials (ERPs) and steady-state visual evoked potentials (SSVEPs), the relevant aspects are already well defined (e.g. temporal in ERPs and frequency related to stimuli in SSVEPs) and are therefore less affected by frequency-related subject variability. This suggests that the practical utility of the suggested approach may depend on the target paradigm and that task-specific adaptations might be required for optimal performance across different EEG contexts.

Finally, although no significant correlations with MAAS scores were observed, this does not necessarily exclude behavioral and neural associations in meditation. One possible explanation is that the MAAS primarily measures a default mindfulness trait rather than the active meditative state. Future work could consider alternative behavioral measures, such as experience sampling or meditation depth rating scales, which may provide more direct and sensitive correlates of neural decoding performance.

5. Conclusion

This work addresses the challenge of subject variability in EEG-based meditation decoding by creating a subject-agnostic model for classifying rest versus meditation states. To achieve this, unsupervised DA techniques were applied. Integrating RSDA and CMMN effectively reduces subject variability,

allowing for a more robust and generalizable classification of meditation versus rest states. In addition, frequency analysis revealed that θ, α, and β bands were sufficient for distinguishing these states, while alternative time-series normalization techniques, such as z-score, provided no improvement. Evaluations of smaller EEG setups showed that frontopolar and parietal regions, when combined with the proposed alignment method, achieved acceptable performance, underscoring their potential for real-world applications.

To conclude, this work highlights the significance of combining spatial and temporal alignment techniques for improving EEG-based meditation decoding. This lays the foundation for robust neurofeedback applications that can effectively support meditation practice across diverse subjects to support anxiety and stress regulation in everyday settings and as an adjunct to care.

Data availability statement

No new data were created or analysed in this study.

Acknowledgments

The authors would like to acknowledge Dr Thomas Strypsteen for his scientific input. Research is supported by Fonds voor Wetenschappelijk Onderzoek—Vlaanderen (FWO) Grants G046321N, G046925N and K222423N and the Internal KU Leuven funds IDN/21/022. This research received funding from the Flemish Government (AI Research Program).

ORCID iDs

Angeliki-Ilektra Karaiskou 0000-0001-7982-1941
Carolina Varon 0000-0002-9581-0676
Kaat Alaerts 0000-0001-8665-6374
Maarten De Vos 0000-0002-3482-5145

References

[1] Reynolds P 2021 Easing burnout in health care *IEEE Pulse* **12** 19–22
[2] Goyal M *et al* 2014 Meditation programs for psychological stress and well-being: a systematic review and meta-analysis *JAMA Intern. Med.* **174** 357–68
[3] Brandmeyer T and Delorme A 2018 Reduced mind wandering in experienced meditators and associated EEG correlates *Exp. Brain Res.* **236** 2519–28
[4] Kuriakose S S, Swamy A, Venugopal R and Sasidharan A 2022 Simple Neurofeedback via Machine Learning: challenges in real time multivariate assessment of meditation state *bioRxiv* (https://doi.org/10.1101/2022.09.27.509655)
[5] Pandey P, Rodriguez-Larios J, Miyapuram K P and Lomas D 2023 Detecting moments of distraction during meditation practice based on changes in the EEG signal *2023 IEEE Applied Sensing Conf. (APSCON)* (IEEE) pp 1–3
[6] Lawhern V J, Solon A J, Waytowich N R, Gordon S M, Hung C P and Lance B J 2018 EEGNet: a compact convolutional neural network for EEG -based brain–computer interfaces *J. Neural Eng.* **15** 056013
[7] Schirrmeister R T, Springenberg J T, Fiederer L D J, Glasstetter M, Eggensperger K, Tangermann M, Hutter F, Burgard W and Ball T 2017 Deep learning with convolutional neural networks for EEG decoding and visualization *Hum. Brain Mapp.* **38** 5391–420
[8] Heilmeyer F A, Schirrmeister R T, Fiederer L D J, Volker M, Behncke J and Ball T 2018 A large-scale evaluation framework for EEG deep learning architectures *2018 IEEE Int. Conf. on Systems, Man and Cybernetics (SMC)* (IEEE) pp 1039–45
[9] Karaiskou A-I, Varon C, Alaerts K and De Vos M 2023 Cross-subject mindfulness meditation EEG decoding *2023 IEEE Int. Conf. on Metrology for EXtended Reality, Artificial Intelligence and Neural Engineering (MetroXRAINE)* (IEEE) pp 781–6
[10] Hosseini S and Guo X 2019 Deep convolutional neural network for automated detection of mind wandering using EEG signals *Proc. 10th ACM International Conference on Bioinformatics, Computational Biology and Health Informatics* (Association for Computing Machinery) pp 314–9
[11] Jin C Y, Borst J P and van Vugt M K 2023 Decoding study-independent mind-wandering from EEG using convolutional neural networks *J. Neural Eng.* **20** 026024
[12] Kostas D and Rudzicz F 2020 Thinker invariance: enabling deep neural networks for BCI across more people *J. Neural Eng.* **17** 056008
[13] Raza H, Rathee D, Zhou S-M, Cecotti H and Prasad G 2019 Covariate shift estimation based adaptive ensemble learning for handling non-stationarity in motor imagery related EEG-based brain-computer interface *Neurocomputing* **343** 154–66
[14] Altindis F, Banerjee A, Phlypo R, Yilmaz B and Congedo M 2023 Transfer learning for P300 brain-computer interfaces by joint alignment of feature vectors *IEEE J. Biomed. Health Inf.* **27** 4696–706
[15] Zoumpourlis G and Patras I 2024 Motor imagery decoding using ensemble curriculum learning and collaborative training *2024 12th IEEE Int. Winter Conf. on Brain-Computer Interface (BCI)* (IEEE) pp 1–7
[16] He H and Wu D 2020 Transfer learning for brain—computer interfaces: a euclidean space data alignment approach *IEEE Trans. Biomed. Eng.* **67** 399–410
[17] Junqueira B, Aristimunha B, Chevallier S and de Camargo R Y 2024 A systematic evaluation of euclidean alignment with deep learning for EEG decoding *J. Neural Eng.* **21** 036038
[18] Xu L, Xu M, Ke Y, An X, Liu S and Ming D 2020 Cross-dataset variability problem in EEG decoding with deep learning *Front. Hum. Neurosci.* **14** 103
[19] Rodrigues P L C, Jutten C and Congedo M 2019 Riemannian procrustes analysis: transfer learning for brain—computer interfaces *IEEE Trans. Biomed. Eng.* **66** 2390–401
[20] Mellot A, Collas A, Rodrigues P L C, Engemann D and Gramfort A 2023 Harmonizing and aligning M/EEG datasets with covariance-based techniques to enhance predictive regression modeling *Imaging Neurosci.* **1** 1–23
[21] Gnassounou T, Flamary R and Gramfort A 2023 Convolution Monge mapping normalization for learning on sleep data *Advances in Neural Information Processing Systems* vol 36 (available at: https://proceedings.neurips.cc/paper_files/paper/2023/file/21718991f6acf19a42376b5c7a8668c5-Paper-Conference.pdf)

[22] Donoghue T et al 2020 Parameterizing neural power spectra into periodic and aperiodic components Nat. Neurosci. 23 1655–65
[23] Apicella A, Isgrò F, Pollastro A and Prevete R 2023 On the effects of data normalization for domain adaptation on EEG data Eng. Appl. Artif. Intell. 123 106205
[24] Zanini P, Congedo M, Jutten C, Said S and Berthoumieu Y 2018 Transfer learning: a Riemannian geometry framework with applications to brain—computer interfaces IEEE Trans. Biomed. Eng. 65 1107–16
[25] Rodriguez-Larios J, de Oca E A B M and Alaerts K 2021 The EEG spectral properties of meditation and mind wandering differ between experienced meditators and novices Neuroimage 245 118669
[26] Kabat-Zinn J and Hanh T N 2013 Full Catastrophe Living: Using the Wisdom of Your Body and Mind to Face Stress, Pain and Illness (BANTAM) pp 722
[27] Brown K W and Ryan R M 2003 The benefits of being present: mindfulness and its role in psychological well-being J. Personality Soc. Psychol. 84 822
[28] Holm S 1979 A simple sequentially rejective multiple test procedure Scand. J. Stat. 6 65–70 (available at: www.jstor.org/stable/4615733)
[29] Combrisson E and Jerbi K 2015 Exceeding chance level by chance: the caveat of theoretical chance levels in brain signal classification and statistical assessment of decoding accuracy J. Neurosci. Methods 250 126–36
[30] Muthukumaraswamy S D 2013 High-frequency brain activity and muscle artifacts in MEG/EEG: a review and recommendations Front. Hum. Neurosci. 7 138
[31] Engel A K and Fries P 2010 Beta-band oscillations—signalling the status quo? Curr. Opin. Neurobiol. 20 156–65
[32] Lee D J, Kulubya E, Goldin P, Goodarzi A and Girgis F 2018 Review of the neural oscillations underlying meditation Front. Neurosci. 12 178
[33] Brandmeyer T and Delorme A 2021 Meditation and the wandering mind: a theoretical framework of underlying neurocognitive mechanisms Perspect. Psychol. Sci. 16 39–66
[34] Zhang Z, Luh W-M, Duan W, Zhou G D, Weinschenk G, Anderson A K and Dai W 2021 Longitudinal effects of meditation on brain resting-state functional connectivity Sci. Rep. 11 11361
[35] Kaur C and Singh P 2015 EEG derived neuronal dynamics during meditation: progress and challenges Adv. Prev. Med. 2015 614723
[36] Fox K C, Dixon M L, Nijeboer S, Girn M, Floman J L, Lifshitz M, Ellamil M, Sedlmeier P and Christoff K 2016 Functional neuroanatomy of meditation: a review and meta-analysis of 78 functional neuroimaging investigations Neurosci. Biobehav. Rev. 65 208–28
[37] Yordanova J, Kolev V, Nicolardi V, Simione L, Mauro F, Garberi P, Raffone A and Malinowski P 2021 Attentional and cognitive monitoring brain networks in long-term meditators depend on meditation states and expertise Sci. Rep. 11 4909
[38] Acharya S, Khosravi A, Creighton D, Alizadehsani R and Acharya U R 2025 Neurostressology: a systematic review of EEG-based automated mental stress perspectives Inform. Fusion 124 103368
[39] Hinss M F, Darmet L, Somon B, Jahanpour E, Lotte F, Ladouce S and Roy R N 2021 An EEG Dataset for Cross-Session Mental Workload Estimation: Passive BCI Competition of the Neuroergonomics Conf. 2021 (https://doi.org/10.5281/zenodo.4917218)
[40] Singh G, Chanel C P and Roy R N 2021 Mental workload estimation based on physiological features for pilot-UAV teaming applications Front. Hum. Neurosci. 15 692878
[41] She Q, Shi X, Fang F, Ma Y and Zhang Y 2023 Cross-subject EEG emotion recognition using multi-source domain manifold feature selection Comput. Biol. Med. 159 106860
[42] Gnassounou T, Collas A, Flamary R, Lounici K and Gramfort A 2024 Multi-source and test-time domain adaptation on multivariate signals using spatio-temporal Monge alignment (arXiv:2407.14303)